

MAGNETOSTRICTION WITH MICHELSON INTERFEROMETER

*A project report Submitted
in Partial Fulfilment of the Credits
for the Course of
Intgrated Physics Lab II*

by
MAITREY SHARMA



to the
School of Physical Sciences
National Institute of Science Education and Research
Bhubaneswar
March 14, 2023

ABSTRACT

Magnetostriction is a property exhibited by magnetic materials that causes them to change their shape or dimensions during the process of magnetization. This report investigates the phenomena of magnetostriction in the rods of Nickel, Iron and Copper by using a Michelson interferometer setup. The results showed that the magnetostriction effect was present in both Ni and Fe rods but absent in the Copper rod. Further, the effect of altering the arm lengths of the interferometer was examined. The effectiveness of this setup to study magnetostrictive effects was also discussed. Instruments interfaced with a LabVIEW program were used to record and export the data.

Contents

1	Introduction	1
1.1	Objectives	2
2	Theory	3
2.1	Magnetostriction	3
2.2	LASER	4
2.3	Michelson Interferometer	5
2.4	Photo-diode Detector	7
3	Experimental Set-up	9
4	Experiments and Analysis	13
4.1	With Iron	13
4.2	With Nickel	13
4.3	With Copper	13
5	Extensions and Innovation	19
5.1	With Iron	19
5.2	With Nickel	19
6	Results and Discussion	25
7	Summary and Conclusions	27
	Bibliography	28

Chapter 1

Introduction

In the early 1800s, the study of electricity and magnetism was a burgeoning field, full of exciting discoveries and new insights. Hailing from Lancashire, English physicist James Joule, namesake for the SI unit of energy and heat, was studying the ways in which magnetic fields interacted with matter. He had already made a name for himself in the scientific community for his work on the relationship between heat and energy, but he was eager to explore the ways in which magnets could affect the behavior of materials.

In 1842, Joule made a groundbreaking discovery that would change the course of his research and contribute to the development of a new field of study: magnetostriction. While experimenting with a sample of iron that had been placed in a magnetic field, Joule noticed something peculiar. As he varied the strength of the field, he observed that the iron sample actually changed in size. When the field was turned off, the sample returned to its original dimensions.

Joule was fascinated by this behavior and began to explore it in more detail. He found that other materials, including nickel and cobalt, exhibited similar properties under the influence of a magnetic field. He called this phenomenon “magnetostriction,” from the Greek words for “magnet” and “to twist.”

Joule’s discovery opened up a whole new area of research, as scientists sought to understand the underlying mechanisms behind magnetostriction and explore its potential applications. Over time, they discovered that magnetostriction was closely related to other magnetic effects, such as the magneto-optic effect and the giant

magnetoresistance effect. Today, magnetostriction continues to be an active area of research, with applications in fields ranging from materials science to electrical engineering as it allows storing electrical energy in form of mechanical energy at scale.

In this term report, we used a Michelson interferometer setup paired with a He-Ne laser to study this phenomena.

1.1 Objectives

The following objectives were formulated and achieved for this experiment:

1. To study the phenomena of magnetostriction in Nickel, Iron and Copper rods.
2. To measure longitudinal strain with the applied varying magnetic field.

Chapter 2

Theory

In this chapter, the theoretical background will be detailed before we discuss the particulars of the experiment.

2.1 Magnetostriiction

The internal structure of ferromagnetic materials is composed of domains, each of which is a region of uniform magnetization. The domain boundaries move and the domains rotate when a magnetic field is applied; both of these effects change the material's dimensions. Because it requires more energy to magnetize a crystalline material in one direction than in another, magnetocrystalline anisotropy¹ is the reason that altering a material's magnetic domains causes a change in the material's dimensions. The material will tend to rearrange its structure so that an easy axis is aligned with the field to minimize the free energy of the system if a magnetic field is applied to it at an angle to an easy axis of magnetization². This differential induction of direction leads to strain in the material.

In fact, the reciprocal effect is also observed in the form of Villari effect, which is defined as the change in the magnetic susceptibility (which quantifies the response to an applied field) of a magnetic material under some form of mechanical stress. The Matteucci and Wiedemann effects are also two related phenomena where mechanical transformation of ferromagnetic materials leads to changes in their magnetic

¹A ferromagnetic material is said to have magnetocrystalline anisotropy if it takes more energy to magnetize it in certain directions than in others.

²Easy axis refers to the energetically favorable direction of the spontaneous magnetization in a ferromagnetic material.

properties.

The changes in dimensions of the material are always in the direction of magnetization, and it they can be positive or negative depending on if the material is contracting or elongating. The distortions are usually of the order 10^{-8} to 10^{-4}m , is due to spin-orbit mutual potential energy and is a function of the direction of magnetisation and the interatomic distances.

2.2 LASER

A laser is a device that emits a narrow beam of coherent light with small angular dispersion. It works on the principle of stimulated emission. The basic concept is to have the electrons in an inverted state where most of them are in the excited levels in a gain medium (crystal or gas). Light is created when this medium is excited by an external energy source (stimulation). This leads to chain reaction where the population inversion reverses and all the electrons fall to the ground level. The photons travel back and forth through a resonant cavity, which contains mirrors at both ends, and are amplified with each pass through the gain medium.

In our experiment, we are using the He-Ne laser. The stimulation is a small electric current and the final colour of the beam produced is red (632.8 nm).

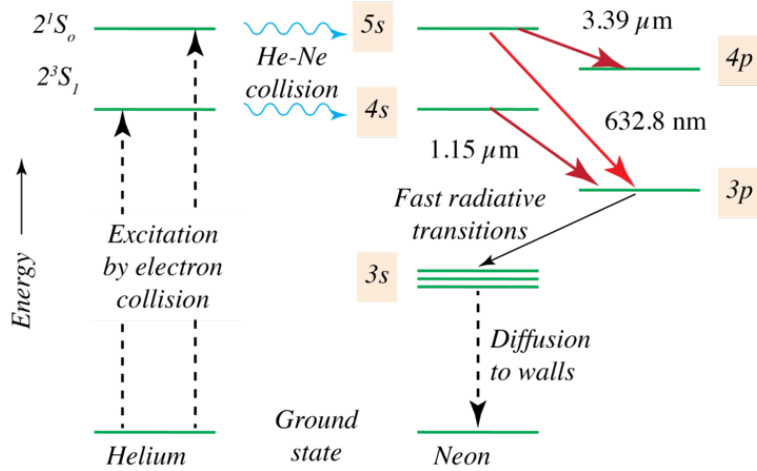


Figure 2.1: Energy Levels in the lasing medium

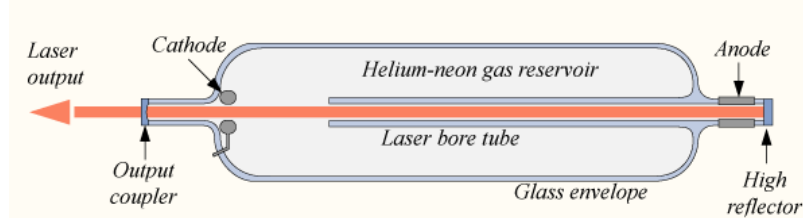


Figure 2.2: Construction of the laser

2.3 Michelson Interferometer

The Michelson interferometer is one of the most important devices that is used to measure small distances.

The basic setup of a Michelson interferometer consists of a beam splitter, two mirrors, and a detector. A beam of light is split by the beam splitter, with half of the light directed towards one mirror and half towards the other mirror. The mirrors reflect the light back towards the beam splitter, where the two beams are recombined. The interference between the two beams produces an interference pattern that can be observed at the detector.

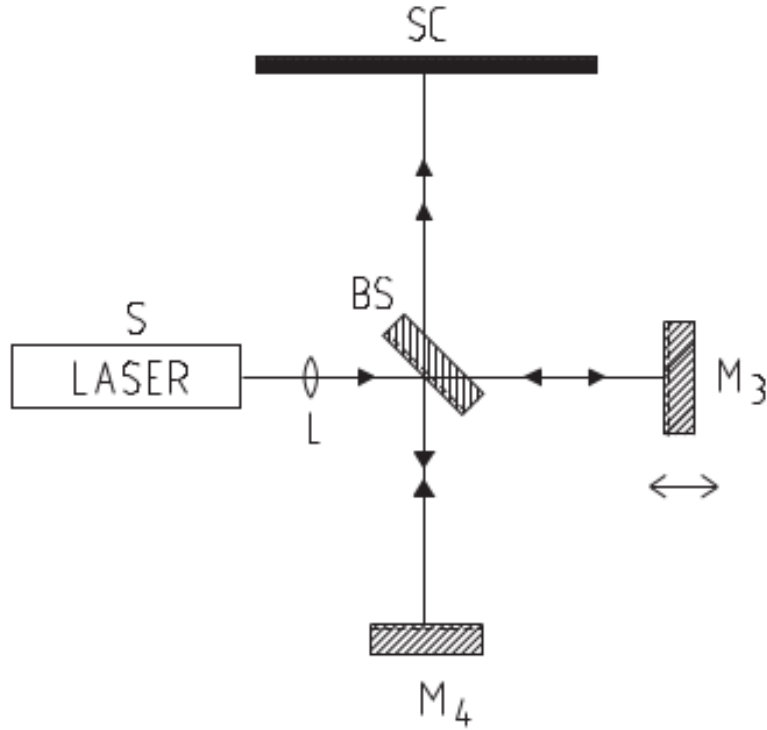


Figure 2.3: Michelson arrangement for Interference. **S** represents the light source; **SC** the detector (or the position of the screen)

By varying the distance between one of the mirrors and the beam splitter, the interference pattern can be changed. This allows the Michelson interferometer to be used for a variety of measurements. By measuring the change in interference pattern as the sample is moved, the length change can be obtained. To obtain the equation for the interference pattern, we use the concept of superposition of waves.

$$2d \cos \theta = m\lambda \quad (2.1)$$

This means that for a given theta, the number of fringes that cross a point depends on how d changes. Hence, we can count the number of fringes changed to find out the change in distance of the mirror.

Magnetostriction can be described thermodynamically using S (elastic tension), s (deformation $\Delta l/l$), B (magnetic induction), H (magnetic field strength), μ (magnetic

permeability) as

$$\frac{1}{\mu} = \frac{\partial H}{\partial B},$$

E (elasticity module) with

$$E = \frac{\partial S}{\partial s},$$

as

$$\frac{\partial S}{\partial s} = \frac{1}{4\pi} \cdot \frac{\partial H}{\partial s} \quad (2.2)$$

2.4 Photo-diode Detector

A photodiode detector is a type of semiconductor device that is used to detect light or optical signals. Photodiode detectors are made from a special type of semiconductor material, such as silicon or germanium, which is doped to create a p-n junction. When light enters the photodiode, it creates electron-hole pairs in the depletion region of the p-n junction. The resulting current that flows through the photodiode is proportional to the amount of light that is detected.



Figure 2.4: Photodiode Detector

If there is a bright fringe incident on the detector, there will be an output voltage signal which can be recorded. In the case of a dark fringe, we will not observe any voltage output.

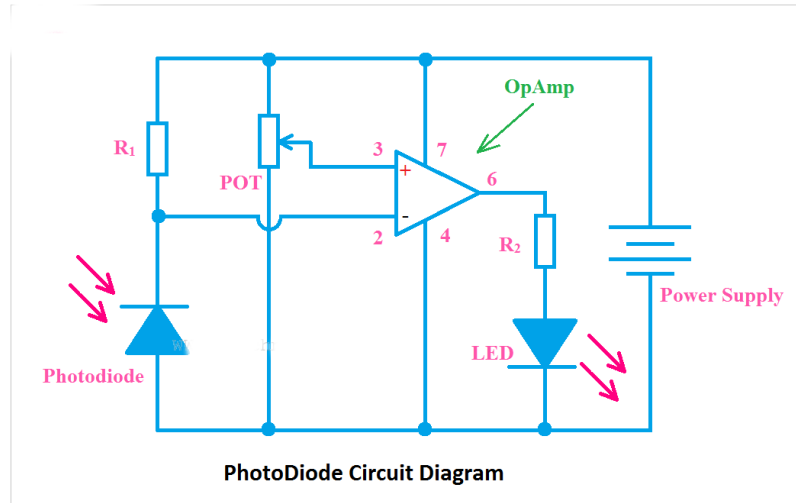


Figure 2.5: Photodiode Detector Circuit with Amplifier

In our particular case, we use an op-amp. Whenever the photodiode senses light, it generates a voltage. In this setup, an op-amp serves as a comparator. It compares the voltage generated by the photodiode to the reference voltage supplied by the V_{cc} or main power supply and produces output accordingly.

Chapter 3

Experimental Set-up

The mirrors utilized in this setup are surface reflecting, which allows the incident beam to exit the mirror at the point of incidence. The laser beam is directed towards the first mirror M1 of the interferometer setup. Mirror M2 redirects the beam towards the beam splitter. The beam splitter transmits half of the radiation to the translatable mirror M3, while reflecting the other half towards the fixed mirror M4. After reflecting from M3, half of the light is directed towards the screen, and the other half from M4 is also transmitted to the screen. The rays from mirrors M3 and M4 interfere behind the glass plate, producing circular fringe patterns. In our experiment, we used a beam expander placed between M2 and the beam splitter to achieve this. When the length of one of the mirror arms changes, the interference pattern also changes, causing the collapse or generation of fringes. Figure 4 shows that the rod with the current coil is attached to mirror M3.

Here for getting more plot points we count the bright and dark fringes which sinks in or source out. So, in the calculations and further discussions n will vary as 0.5, 1, 1.5, 2... Thereby the formula gets modified to:

$$\Delta l = n \frac{\lambda}{4} \quad (3.1)$$

The output of the interferometer falls on a photodetector system that measures the number of fringes that have shifted. A voltage is produced as an output from the photodetector. The output from the photodetector is then connected to a digital multimeter PPH-1503, which is connected to a PC. This PC has Labview software installed where a counting program is written to get the data on shifted fringes.

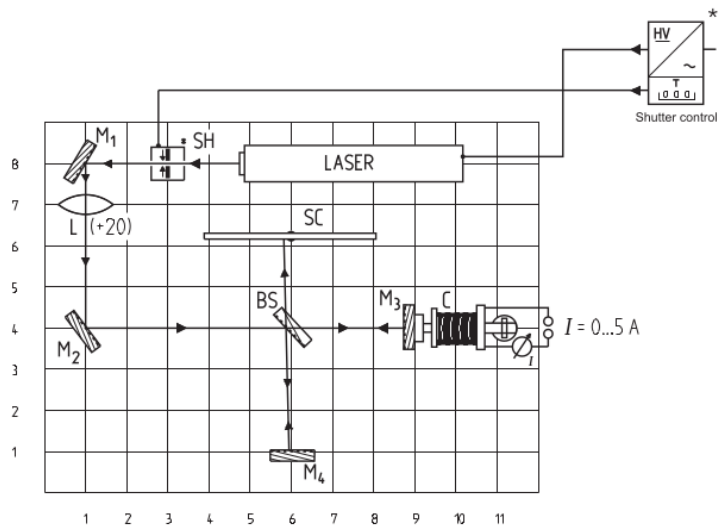


Figure 3.1: Schematic of the experiment on the magnetic bench

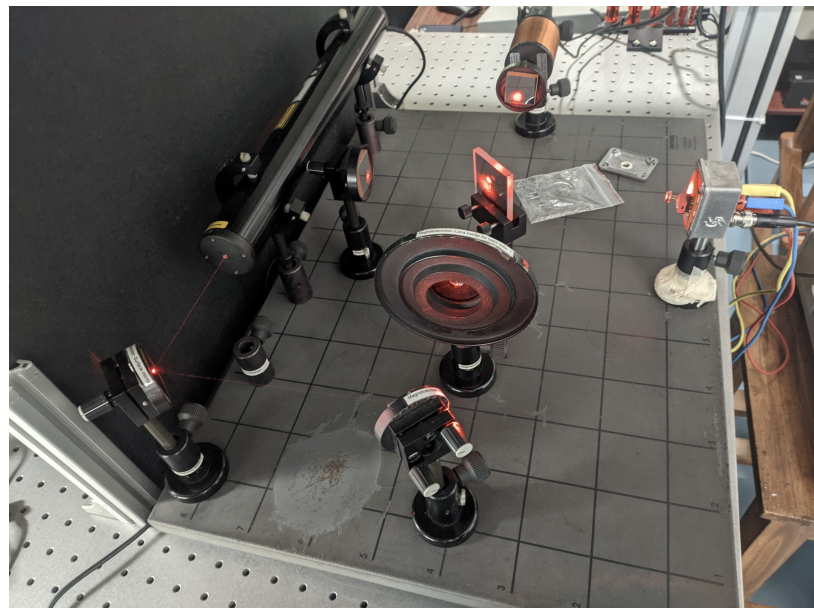


Figure 3.2: Experimental set-up

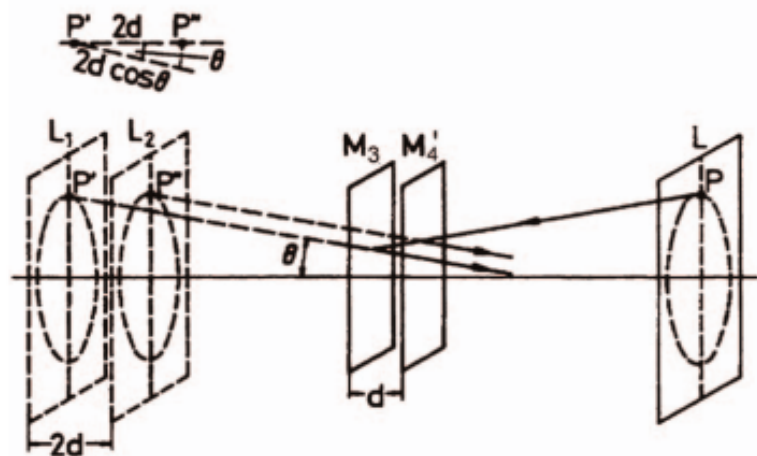


Figure 3.3: Formation of circular interference fringes

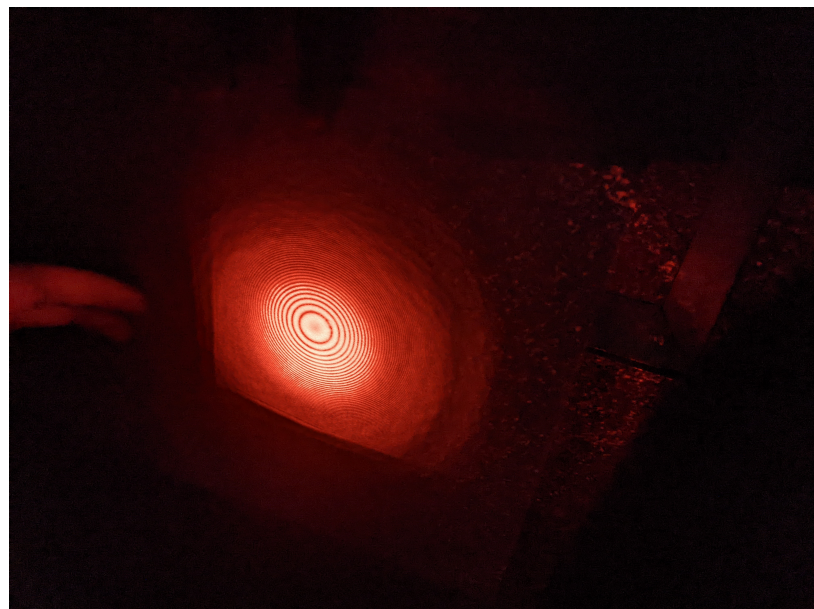


Figure 3.4: Circular fringes observed on the screen after alignment.

This software is also used to regulate the current provided to the coil. The coil is also connected to the PPH-1503 to facilitate this process.

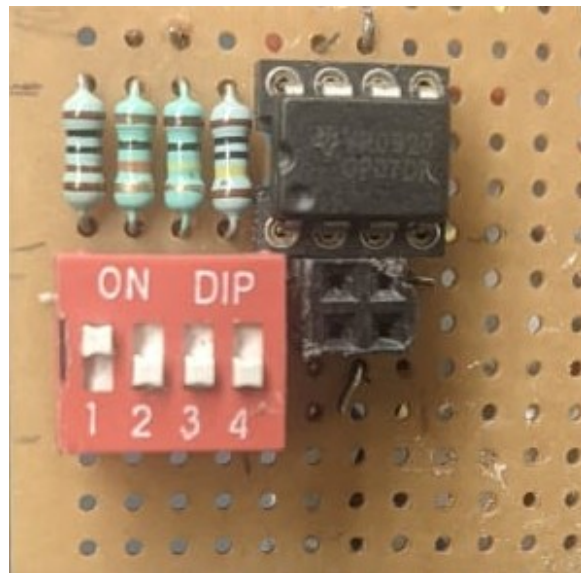


Figure 3.5: Detector Circuit

This entire setup is done on an optical bench which is supported by pneumatic vibration isolators. This allows us to get results which are free from noise.



Figure 3.6: Vibration Isolator

Chapter 4

Experiments and Analysis

4.1 With Iron

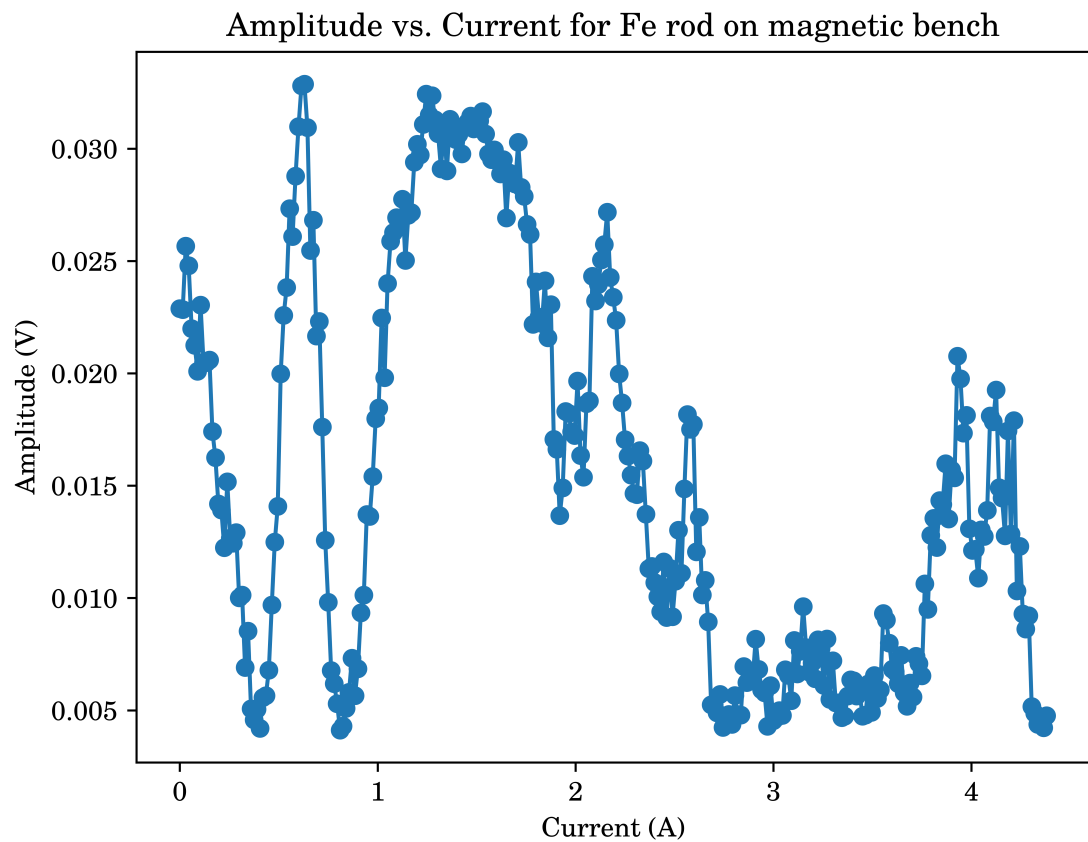


Figure 4.1: The amplitude versus current data obtained for Fe rod on the magnetic bench.

4.2 With Nickel

4.3 With Copper

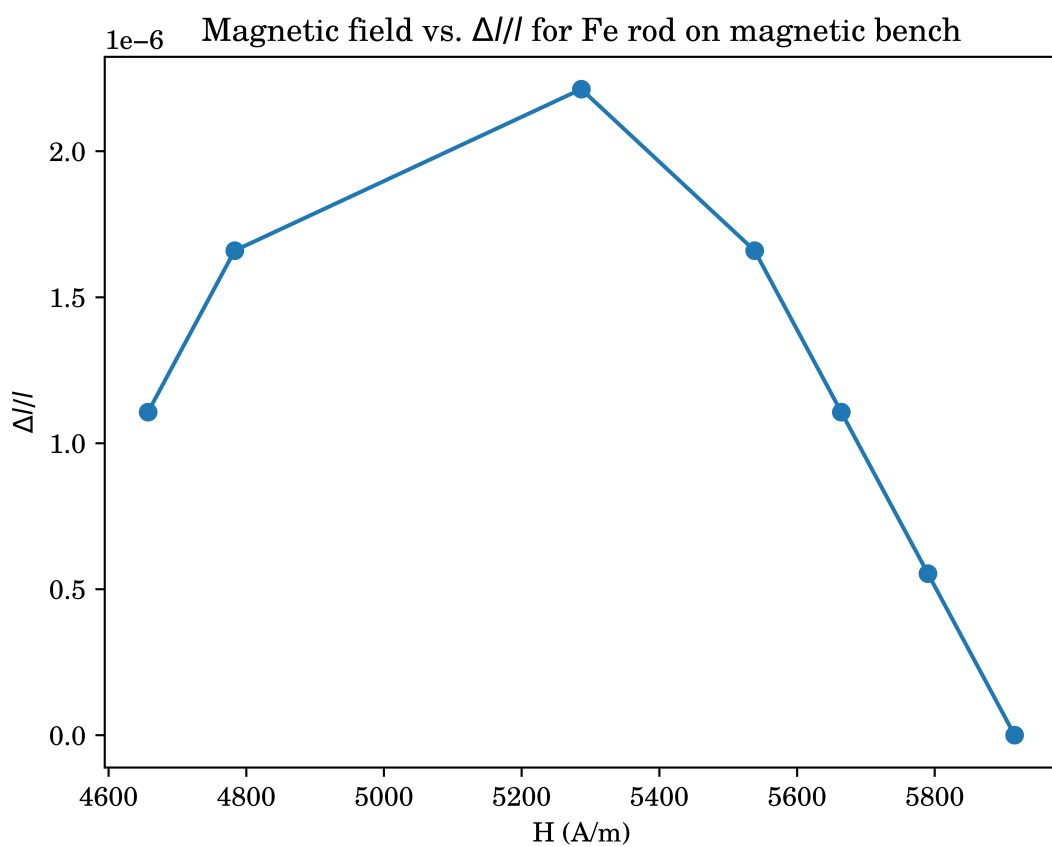


Figure 4.2: The variation in strain with applied magnetic field for Fe on the magnetic bench.

Current (A)	Ring changes (n)	Δl ($\times 10^{-9}$ m)	Magnetization, H (A m $^{-1}$)	$\Delta l/l$ ($\times 10^{-9}$ m)
0.555	1	1.58E-07	4.66E+03	1.11E-06
0.57	1.5	2.37E-07	4.78E+03	1.66E-06
0.63	2	3.16E-07	5.29E+03	2.21E-06
0.66	1.5	2.37E-07	5.54E+03	1.66E-06
0.675	1	1.58E-07	5.66E+03	1.11E-06
0.69	0.5	7.91E-08	5.79E+03	5.53E-07
0.705	0	0.00E+00	5.92E+03	0.00E+00

Table 4.1: The variation in strain with applied magnetic field for Fe on the magnetic bench.

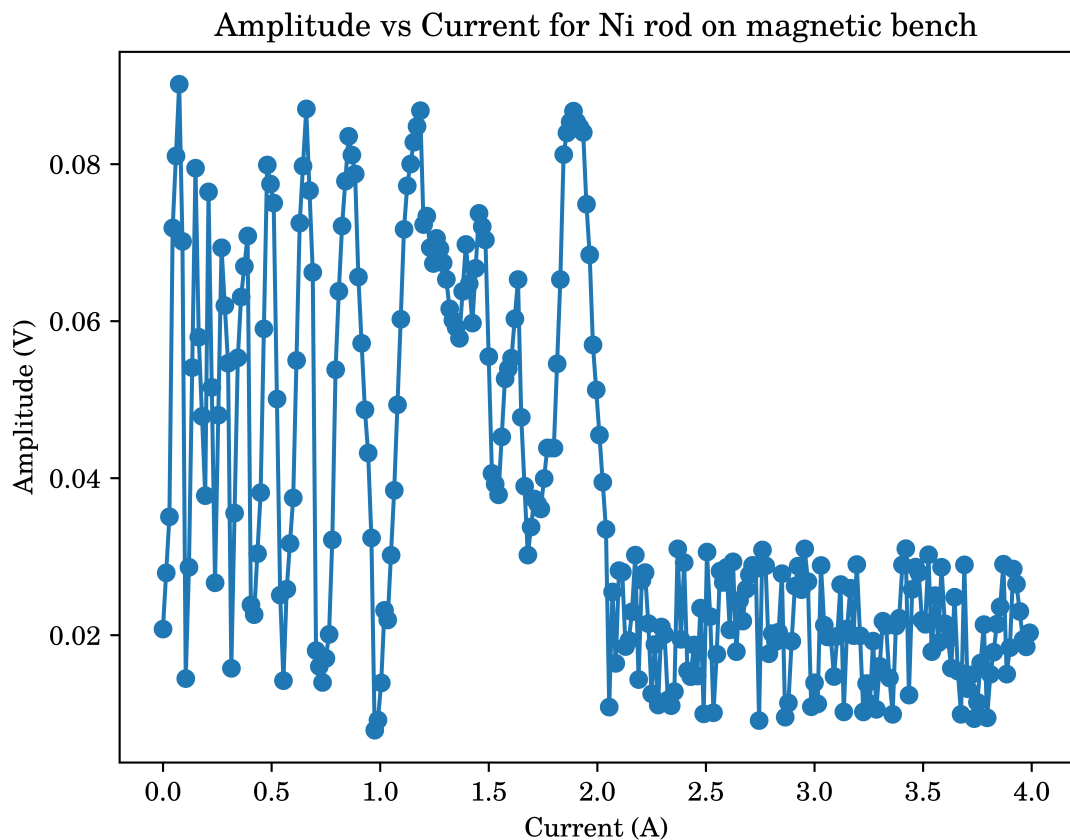


Figure 4.3: The amplitude versus current data obtained for Ni rod on the magnetic bench.

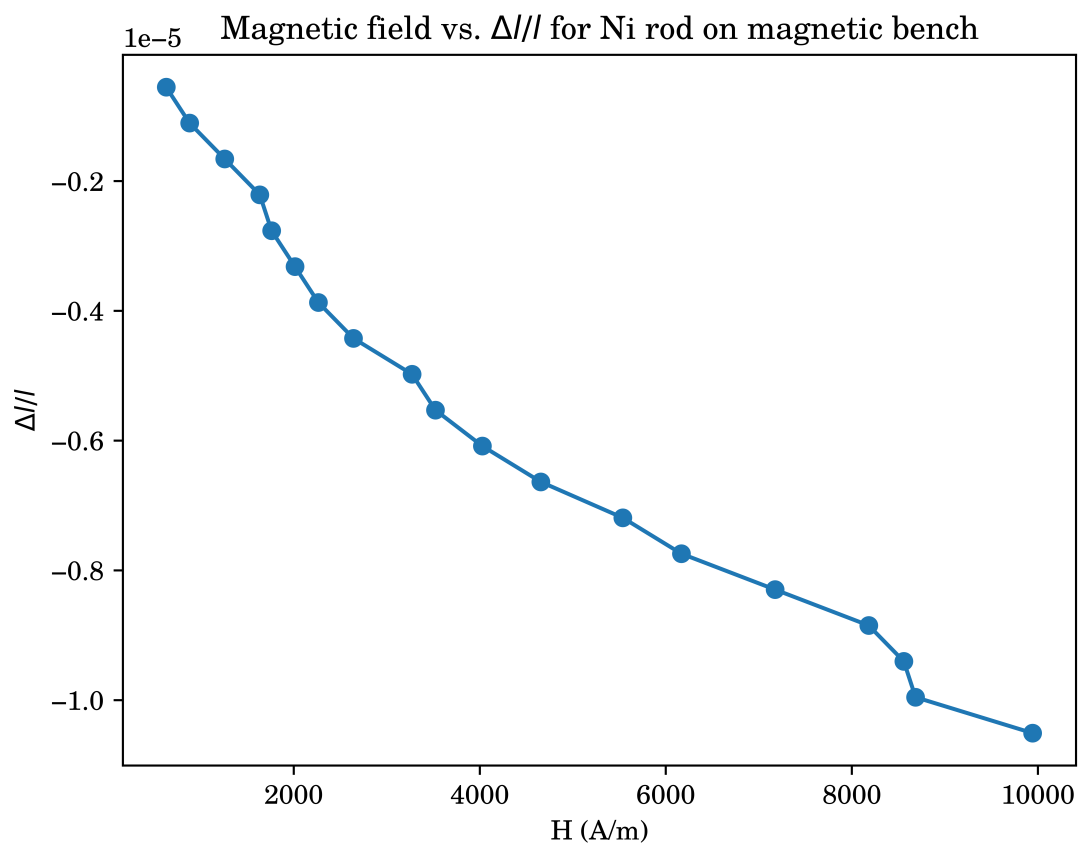


Figure 4.4: The variation in strain with applied magnetic field for Ni on the magnetic bench.

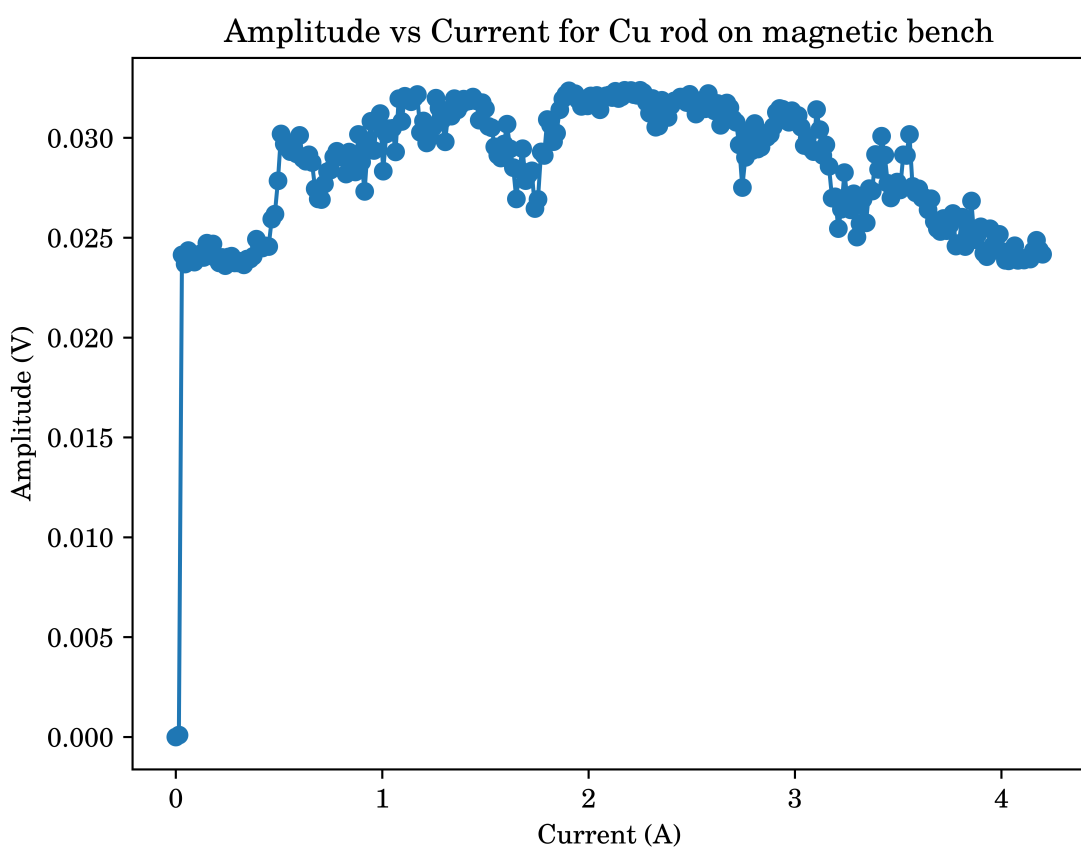


Figure 4.5: The amplitude versus current data obtained for Cu rod on the magnetic bench.

Current (A)	Ring changes (n)	Δl ($\times 10^{-9}$m)	Magnetization, H (A m$^{-1}$)	$\Delta l/l$ ($\times 10^{-9}$m)
0.075	0.5	-7.91E-08	6.29E+02	-5.53E-07
0.105	1	-1.58E-07	8.81E+02	-1.11E-06
0.15	1.5	-2.37E-07	1.26E+03	-1.66E-06
0.195	2	-3.16E-07	1.64E+03	-2.21E-06
0.21	2.5	-3.96E-07	1.76E+03	-2.77E-06
0.24	3	-4.75E-07	2.01E+03	-3.32E-06
0.27	3.5	-5.54E-07	2.27E+03	-3.87E-06
0.315	4	-6.33E-07	2.64E+03	-4.43E-06
0.39	4.5	-7.12E-07	3.27E+03	-4.98E-06
0.42	5	-7.91E-07	3.52E+03	-5.53E-06
0.48	5.5	-8.70E-07	4.03E+03	-6.08E-06
0.555	6	-9.49E-07	4.66E+03	-6.64E-06
0.66	6.5	-1.03E-06	5.54E+03	-7.19E-06
0.735	7	-1.11E-06	6.17E+03	-7.74E-06
0.855	7.5	-1.19E-06	7.17E+03	-8.30E-06
0.975	8	-1.27E-06	8.18E+03	-8.85E-06
1.02	8.5	-1.34E-06	8.56E+03	-9.40E-06
1.035	9	-1.42E-06	8.69E+03	-9.96E-06
1.185	9.5	-1.50E-06	9.94E+03	-1.05E-05

Table 4.2: The variation in strain with applied magnetic field for Ni on the magnetic bench.

Chapter 5

Extensions and Innovation

The first part of our innovation was to transfer the setup from the magnetic optical bench which has been supplied from the equipment manufacturer to an optical breadboard so that we can move beyond the constraints of the limited size of the magnetic breadboard. This has already been covered in the previous section. The optical breadboard enabled us to do much finer adjustments while aligning the interferometer.

The second part of the innovation was to see if changing the arm length of the interferometer would give us better observations. More on why this change in arm length was proposed by us as an innovation is provided in the discussions section. The motivation from this came from the similar use of Michelson interferometer at the LIGO project. The scale of LIGO's instruments is crucial to its search for gravitational waves. The longer the arms of an interferometer, the smaller the measurements they can make. We thought this might improve the resolution and/or accuracy of our results. But later we realized that this did not have much effect on the results. The reasons are discussed in section 6.

5.1 With Iron

5.2 With Nickel

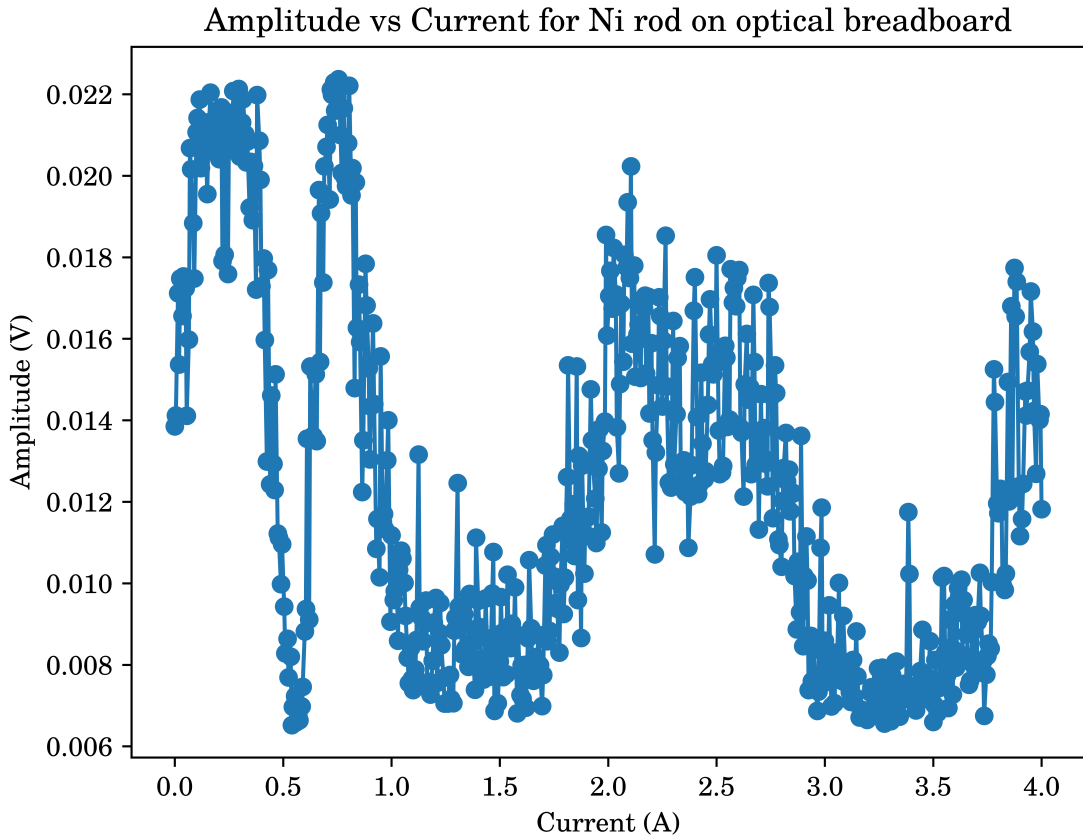


Figure 5.1: The amplitude versus current data obtained for Fe rod on the optical breadboard with altered arm lengths of the interferometer.

Current (A)	Ring changes (n)	Δl ($\times 10^{-9}$ m)	Magnetization, H ($A\ m^{-1}$)	$\Delta l/l$ ($\times 10^{-9}$ m)
0.46	2	3.16E-07	3.86E+03	2.21E-06
0.465	2.5	3.96E-07	3.90E+03	2.77E-06
0.49	3	4.75E-07	4.11E+03	3.32E-06
0.495	2.5	3.96E-07	4.15E+03	2.77E-06
0.51	2	3.16E-07	4.28E+03	2.21E-06
0.52	1.5	2.37E-07	4.36E+03	1.66E-06
0.525	1	1.58E-07	4.41E+03	1.11E-06
0.535	0.5	7.91E-08	4.49E+03	5.53E-07
0.54	0	0.00E+00	4.53E+03	0.00E+00

Table 5.1: The variation in strain with applied magnetic field for Fe on the optical breadboard.

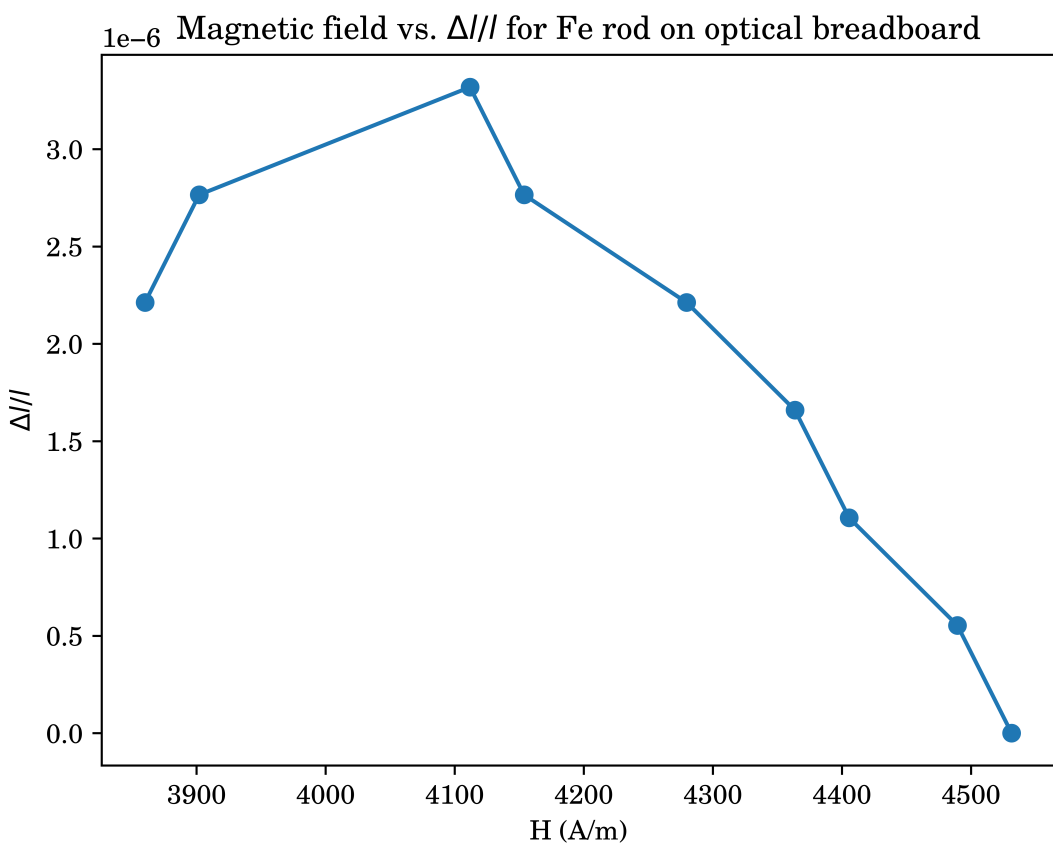


Figure 5.2: The variation in strain with applied magnetic field for Fe on the optical breadboard.

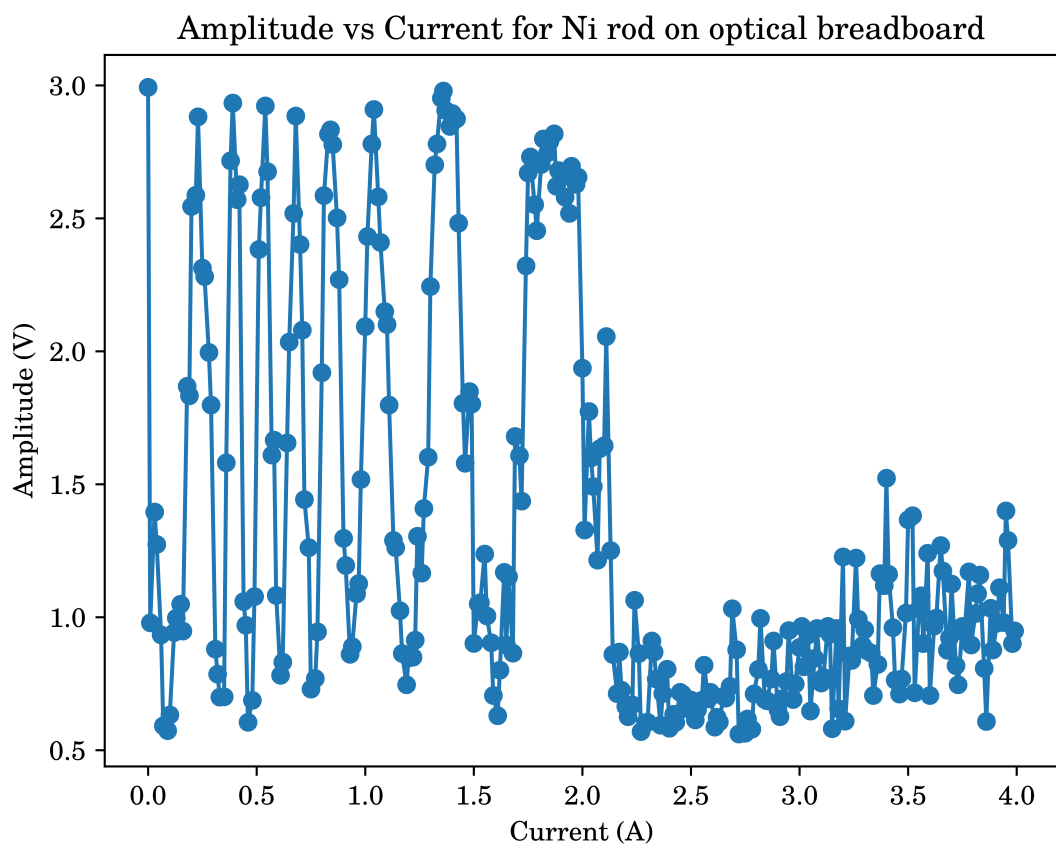


Figure 5.3: The amplitude versus current data obtained for Ni rod on the optical breadboard with altered arm lengths of the interferometer.

Current (A)	Ring changes (n)	Δl ($\times 10^{-9}$m)	Magnetization, H (A m$^{-1}$)	$\Delta l/l$ ($\times 10^{-9}$m)
0.01	0.5	-7.91E-08	8.39E+01	-5.53E-07
0.03	1	-1.58E-07	2.52E+02	-1.11E-06
0.09	1.5	-2.37E-07	7.55E+02	-1.66E-06
0.15	2	-3.16E-07	1.26E+03	-2.21E-06
0.16	2.5	-3.96E-07	1.34E+03	-2.77E-06
0.18	3	-4.75E-07	1.51E+03	-3.32E-06
0.19	3.5	-5.54E-07	1.59E+03	-3.87E-06
0.23	4	-6.33E-07	1.93E+03	-4.43E-06
0.33	4.5	-7.12E-07	2.77E+03	-4.98E-06
0.39	5	-7.91E-07	3.27E+03	-5.53E-06
0.41	5.5	-8.70E-07	3.44E+03	-6.08E-06
0.42	6	-9.49E-07	3.52E+03	-6.64E-06
0.46	6.5	-1.03E-06	3.86E+03	-7.19E-06
0.54	7	-1.11E-06	4.53E+03	-7.74E-06
0.57	7.5	-1.19E-06	4.78E+03	-8.30E-06
0.58	8	-1.27E-06	4.87E+03	-8.85E-06
0.61	8.5	-1.34E-06	5.12E+03	-9.40E-06
0.68	9	-1.42E-06	5.71E+03	-9.96E-06
0.75	9.5	-1.50E-06	6.29E+03	-1.05E-05
0.84	10	-1.58E-06	7.05E+03	-1.11E-05
0.93	10.5	-1.66E-06	7.80E+03	-1.16E-05
1.04	11	-1.74E-06	8.73E+03	-1.22E-05
1.19	11.5	-1.82E-06	9.99E+03	-1.27E-05
1.24	12	-1.90E-06	1.04E+04	-1.33E-05
1.26	12.5	-1.98E-06	1.06E+04	-1.38E-05
1.36	13	-2.06E-06	1.14E+04	-1.44E-05
1.39	13.5	-2.14E-06	1.17E+04	-1.49E-05
1.4	14	-2.21E-06	1.17E+04	-1.55E-05
1.46	14.5	-2.29E-06	1.23E+04	-1.60E-05
1.48	15	-2.37E-06	1.24E+04	-1.66E-05

Table 5.2: The variation in strain with applied magnetic field for Ni on the optical breadboard.

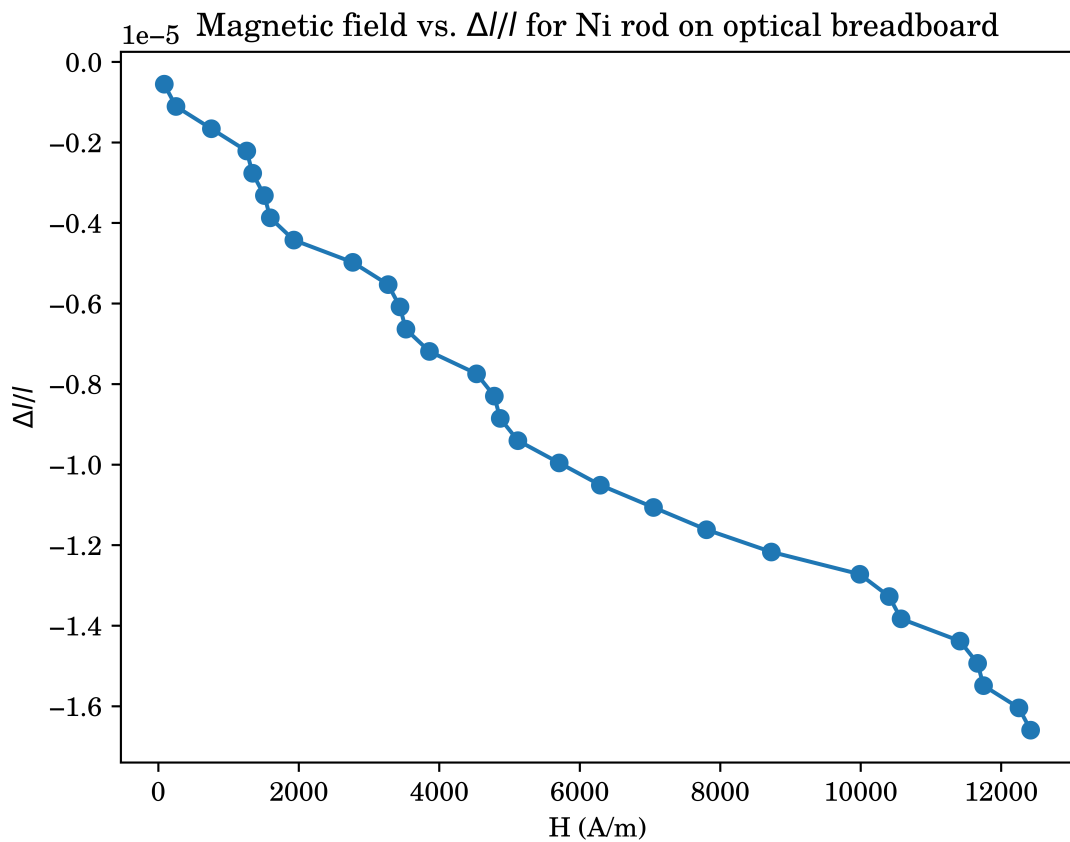


Figure 5.4: The variation in strain with applied magnetic field for Ni on the optical breadboard.

Chapter 6

Results and Discussion

1. An interference pattern was observed.
2. Magnetostriction coefficients were measured in a magnetic optical bench with a standard arm length for Fe, Ni, and Cu. The results showed that Fe had a coefficient of $(1.38 \pm 0.58) \times 10^{-6}$, Ni had a coefficient of $(-5.53 \pm 3.1) \times 10^{-6}$, and Cu did not show any magnetostriction.
3. Magnetostriction coefficients were measured in a mechanical optical bench with an extended arm length for Fe, Ni, and Cu. The results showed that Fe had a coefficient of $(1.84 \pm 1.1) \times 10^{-6}$, Ni had a coefficient of $(-8.57 \pm 4.9) \times 10^{-6}$, and Cu did not show any magnetostriction.
4. These results were in agreement with the literature values.
5. Because Cu is not ferromagnetic, it does not have magnetic domains in the bulk material, and therefore, it was not expected to exhibit any magnetostriction, which was consistent with the observations.
6. The op-amp circuit connected to the photodetector had some loose connections, causing the data to be unreliable. The source of this error was identified, and the loose wires were resoldered to their proper places to rectify the issue.
7. The optical bench experienced vibrations, leading to the disappearance of fringes. To solve this problem, a vibration damping table was utilized to minimize the impact of the vibrations.

8. The laser beam was not aligned with the plane of the optical bench, resulting in the interference not being observed. To fix this issue, a spirit level was used to adjust the beam's position and bring it back into alignment with the plane.
9. The LASER source has a narrow divergence in its beam over a long distance, but a diverging lens was used in the experiment to expand the beam into a circular pattern for ease in counting rings. However, this also meant that the beam could not be used to produce interference patterns for longer arm lengths since the beam would diverge too much to provide relevant data.
10. To overcome this limitation, the lens was removed in the experiment with the longer arm length, and the device was positioned to take readings of standard interference fringes instead of circular fringes.
11. Although a change in arm length should not theoretically affect the observation of fringes, a slight variation in the results was observed. This could be attributed to the fact that the standard interferometer pattern gets less intense after the first few bright fringes, unlike circular fringes, which remain equally bright over a larger region.
12. In future experiments, a Mach-Zehnder interferometer could be used to increase the instrument's accuracy.

Chapter 7

Summary and Conclusions

1. To summarize, the text describes an experiment where interference patterns were observed, and magnetostriction coefficients were measured for Fe, Ni, and Cu using both a magnetic and mechanical optical bench. The results show that Cu did not exhibit any magnetostriction, which was expected due to its non-ferromagnetic nature.
2. During the experiment, the reliability of the data was compromised due to loose connections in the op-amp circuit. Vibrations in the optical bench also led to issues with the fringes, which were resolved by utilizing a vibration damping table. Additionally, the laser beam was not in the right position, and the interference was not observed, but this was rectified by adjusting the beam's position using a spirit level.
3. The experiment used a LASER source with a narrow beam divergence, which was expanded into a circular pattern using a diverging lens for ease in counting rings. However, this limited the experiment's ability to produce interference patterns for longer arm lengths. To overcome this, the lens was removed for the longer arm experiment, and standard interference fringes were observed instead of circular fringes. Despite a slight variation in the results, a Mach-Zehnder interferometer could be used in future experiments to increase the instrument's accuracy.

Bibliography

1. G. Giampieri, R. W. Hellings, M. Tinto, J. E. Faller, *Optics Communications* **123**, 669–678, ISSN: 00304018, (2023; <https://linkinghub.elsevier.com/retrieve/pii/0030401895006117>) (Feb. 1996).
2. T. Kwaaitaal, *Journal of Magnetism and Magnetic Materials* **6**, 290–294, ISSN: 03048853, (2023; <https://linkinghub.elsevier.com/retrieve/pii/0304885377901305>) (Aug. 1977).
3. *LIGO's Interferometer*, LIGO Lab — Caltech (2023; <https://www.ligo.caltech.edu/page/ligos-ifo>).
4. T. Nakata, N. Takahashi, M. Nakano, K. Muramatsu, P. Miyake, *IEEE Transactions on Magnetics* **30**, 4563–4565, ISSN: 00189464, (2023; <http://ieeexplore.ieee.org/document/334149/>) (Nov. 1994).
5. Y.-g. Xu, X.-g. Chen, *Journal of Alloys and Compounds* **582**, 364–368, ISSN: 09258388, (2023; <https://linkinghub.elsevier.com/retrieve/pii/S0925838813019300>) (Jan. 2014).
6. S. Yanase, K. Yamamoto, Y. Okazaki, *Journal of Materials Processing Technology* **108**, 221–224, ISSN: 09240136, (2023; <https://linkinghub.elsevier.com/retrieve/pii/S0924013600007597>) (Jan. 2001).